Current Research (2009) Newfoundland and Labrador Department of Natural Resources Geological Survey, Report 09-1, pages 1-12

THE POINT ROUSSE LISTVENITES, BAIE VERTE, NEWFOUNDLAND: ALTERED ULTRAMAFIC ROCKS WITH POTENTIAL FOR GOLD MINERALIZATION?

M.P. Escayola, J.A. Proenza, C. van Staal, N. Rogers* and T. Skulski
Geological Survey of Canada, 601 Booth Street, Ottawa, ON, K1A 0E8
Corresponding author: *nrogers@nrcan.gc.ca

ABSTRACT

The Point Rousse listvenites of the Baie Verte ophiolite belt, northern Newfoundland, are potential sites of gold mineralization. They are interpreted to have been formed during obduction-related deformation and the accompanying hydrothermal alteration of ultramafic rocks. These unusual rocks have much in common with those from other altered serpentinite-associated gold deposits. Mineralized listvenites display widely varying morphologies and metallic mineral assemblages, but all examples are intimately related to fault zones that bound slices and blocks of carbonatized ophiolite.

Several stages of hydrothermal alteration have been recognized in the Point Rousse listvenites. The hydrothermal mineral assemblages are controlled largely by temperature, X_{CO2}, and oxygen and sulphur fugacity. The transformation of the rocks to talc–carbonate schists (listvenites) by Ca-CO_2-S and As-rich solutions liberated large quantities of silica that were subsequently mobilized and re-deposited to form silicified rocks and quartz-vein networks.

High-magnesian chlorites found in the listvenites have estimated formation temperatures of circa *200°C, which are consistent with the presence of pyrite and millerite in listvenites and birbirites (silicified ultramafic rocks). Gold that is present in trace amounts in some of the sulphides in the ultramafic–mafic rocks, appears to have been mobilized and deposited during hydrothermal alteration, during several deformational stages. The Point Rousse listvenites and their associated Au mineralization are a subject of interest for future research, and also for mineral exploration in the area.*

INTRODUCTION

One of the most important aspects of mineral exploration is the recognition of distinct rock types that form markers for economically significant minerals. Amongst these, rocks recording hydrothermal alteration and metasomatism are perhaps the most valuable. Hydrothermal and metasomatic alteration products are a function both of the mineralogy of the original rocks and subsequent fluid-rock interactions. The influence of hydrothermal fluids in terranes composed of ultramafic rocks results in a wide spectrum of metasomatic rocks, including the distinctive association termed ‘listvenite’. Listvenite, *sensu stricto*, consists mostly of quartz, carbonate and chromium-rich mica that formed in response to the carbonatization of ultramafic and/or ophiolitic rocks. They are commonly associated with other metasomatic rocks, including quartz–carbonate rocks, talc–silica–carbonate-rich rocks and serpentine–talc–chlorite–carbonate rocks.

The term listvenite was first introduced by Rose (1837, 1842) to describe the silica–carbonate metasomatic rocks that host gold-bearing quartz lodes from the Listvenaya Gora in the Ural goldfields (sequence is described in Halls *et al.*, 1991). Transliteration from the original Russian has resulted in a number of different spellings for listvenite over the years, including 'listwanite' and 'listwaenite'. This matter was addressed by Halls and Zhao (1995), where they suggested that 'listvenite' should be used because it is the best translation from the Russian of the geographic feature the rocks were named after. Furthermore, as their description was about likely correlative rocks from Ireland, it seems appropriate to follow their nomenclature. Listvenites that are spatially associated with low-temperature Au, Hg, As, Co, and Ni mineralization are the most economically important set of metasomatic rocks derived from ultramafic precursors. The replacement of serpentine and forsterite by stable Mg-carbonate minerals is also of environmental interest because such reactions have the ability to fix anthropogenic

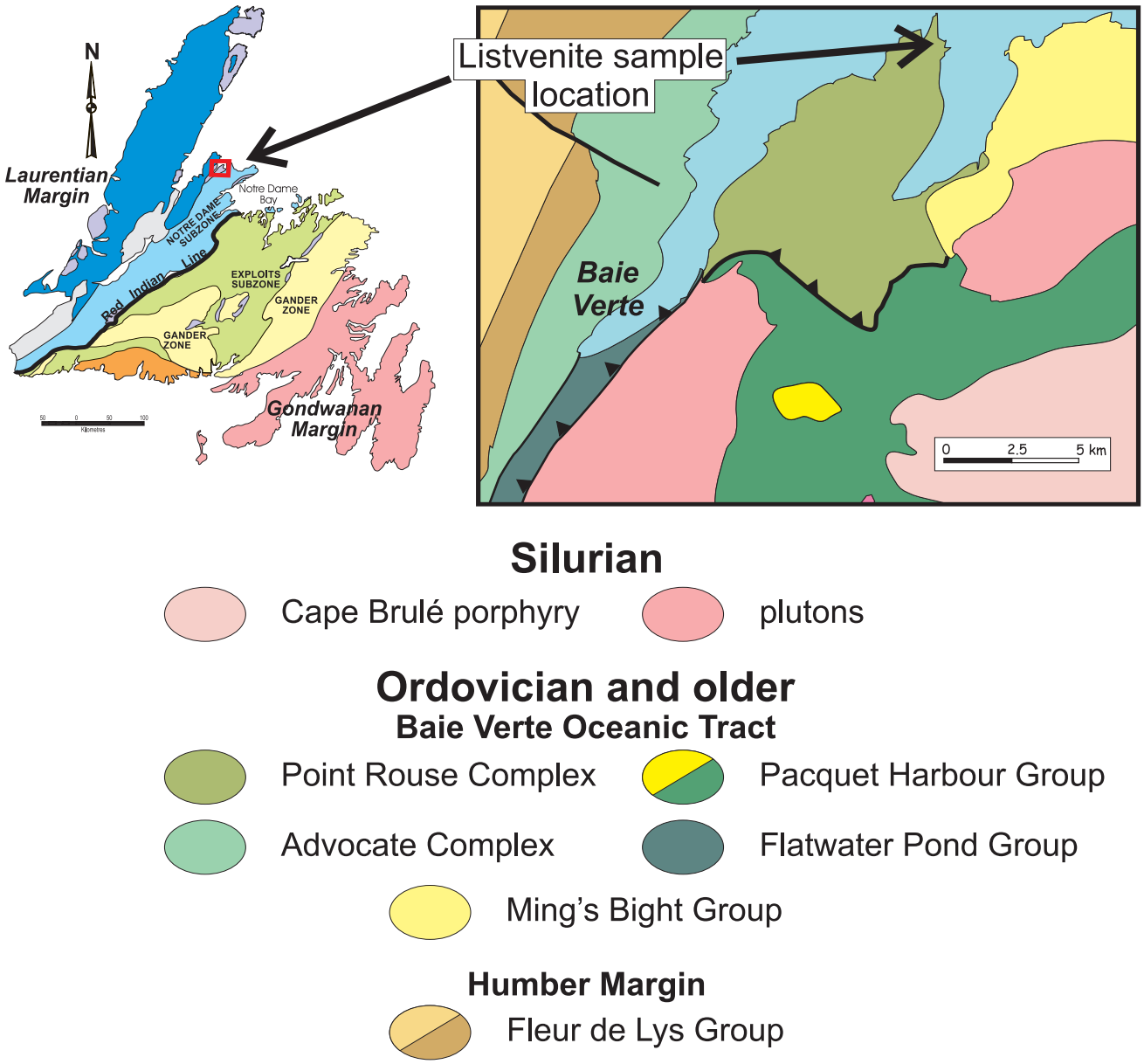

Figure 1. *Location of the Point Rousse complex, Baie Verte Peninsula.*

carbon dioxide (Seifritz, 1990). Globally, carbon sequestration through the process of carbonatization offers virtually unlimited capacity and the promise of safe, permanent storage of CO_2 with little risk of accidental release (Guhthrie *et al.*, 2001; Hansen *et al.*, 2005).

Other mineralized listvenite outcrops occur in the Québec Appalachians known as the Eastern Metals deposit and host Ni–Cu–Zn deposit (Auclair *et al.*, 1993). These occurrences consists of two mineralized areas, a northern Ni–Zn zone and a southern Cu–Ni–Zn–Co–Au–Pt zone. The disseminated and massive sulphides are hosted by intensely carbonatized and silicified rocks at the sheared contacts between serpentinite and graphitic slate.

This study deals with the metasomatic rocks found in the Point Rousse ophiolite, Baie Verte, Newfoundland (Figure 1). This report emphasizes the petrography and mineral geochemistry of the Point Rousse listvenites and their possible mechanism of generation. Future work will be focused on lithogeochemistry and stable isotopes compositions.

GEOLOGY AND FIELD RELATIONS

The Point Rousse complex is part of the Baie Verte ophiolite belt and belongs to the Notre Dame Subzone of the Dunnage Zone of the Newfoundland Appalachians (Figure 1). It consists of variably altered and deformed remnants of an ophiolite suite that are exposed along the Baie

Plate 1. *Point Rousse listvenites outcrops, Baie Verte ophiolite belt, Newfoundland.*

Plate 2. *An outcrop showing characteristics of listvenite breccias.*

Verte–Brompton Line. The Point Rousse complex includes serpentinite, ultramafic cumulates, gabbro, and sheeted diabase dykes, and a supracrustal section of mafic volcanic, volcaniclastic and sedimentary rocks. Listvenites are exposed adjacent to a shear zone related to the Baie Verte–Brompton Line. The shear zone likely formed a pathway for the hydrothermal fluids needed for formation of listvenites. There is still some uncertainty regarding the listvenites in the study area (Plate 1) and their association with dunites or harzburgite cumulates.

Listvenites that occur in the Point Rousse complex are mostly composed of quartz carbonate (ankerite, magnesite and dolomite) and talc, chlorite and/or fuchsite, and are accompanied by disseminated pyrite and other accessory minerals such as chalcopyrite and magnetite. Chromite, which is the most refractory primary mineral in ultramafic rocks, is preserved within the listvenite mineral assemblages (Plate 2).

PETROGRAPHY

Samples were collected from several sites from the Point Rousse. Most of the listvenites are fine- to medium-grained rocks in which no traces of the original mineral assemblage remain. Hand specimens of the sampled rocks have a granular white-flecked appearance due to the mixture of white minerals. Brown-weathered surfaces are caused by the weathering of ankerite/magnesite to limonite (Plate 3).

The listvenites are classified into two broad categories, which are termed ‘silica-poor’ and ‘silica-rich’. The silica-poor listvenites exhibit two mineralogical associations: i) rocks dominated by magnesite–ankerite and chlorite (samples SNB 07 – E01-A02, SNB 07 – E01-B03, SNB 07 – E01-B01, SNB 07 – E01-A02-1, Plate 4); and ii) rocks dom-

Plate 3. *Listvenite appearance caused by the weathering of ankerite to limonite.*

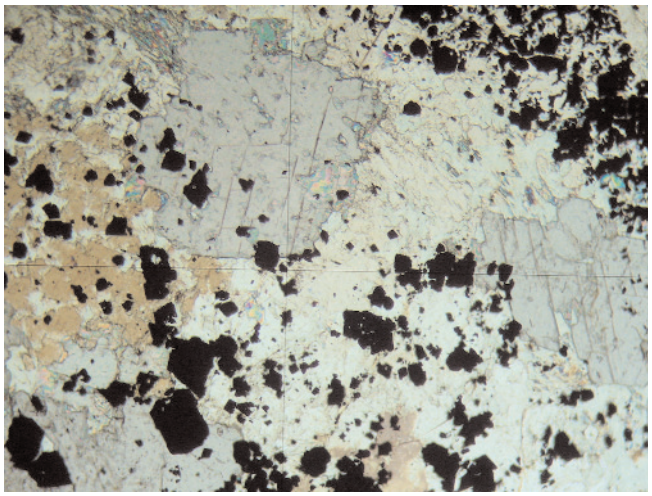

Plate 4. *Ankerite and chlorite.*

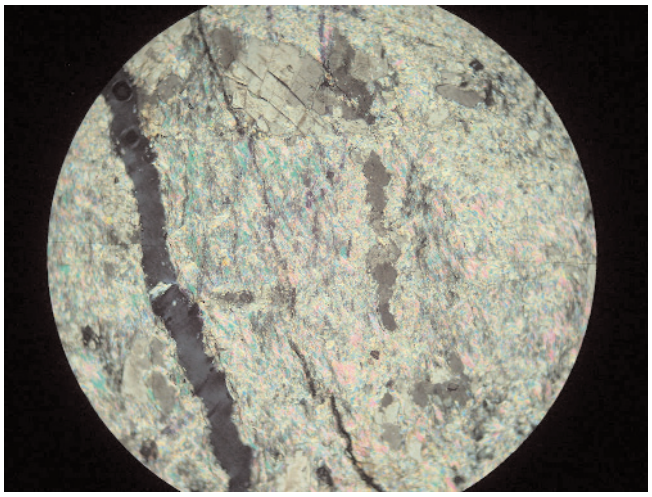

Plate 5. *Dolomite and talc associations.*

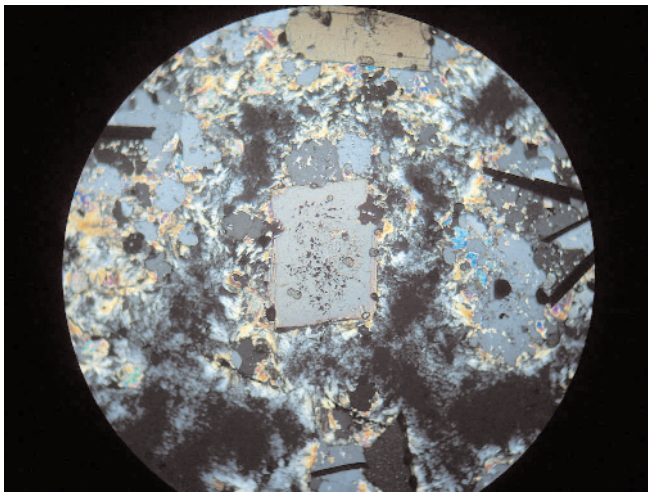

Plate 6. *Birbirite composed of dolomite and talc with quartz.*

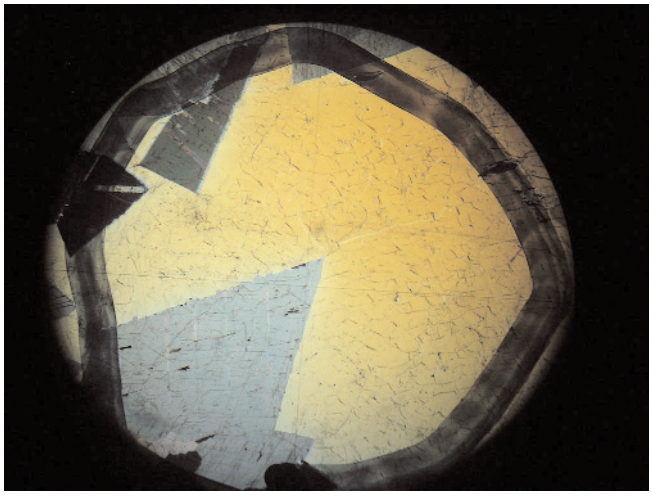

Plate 7. *Quartz in birbirites.*

inated by dolomite, talc, and fuchsite, also containing relict chromite, magnetite and ± pyrite and chalcopyrite (SNB 07 – E01-13, SNB 07 – E01-C01, SNB 07 – E02-A04, SNB 07 – E02-A03, SNB 07 – E 02-A01, SNB 07 – E01-E01, SNB 07 – E01-D01, SNB 07 – E01A-03; Plate 5).

The silica-rich listvenite is composed of dolomite, talc and quartz. This rock type is locally intruded by secondary quartz veins that are rich in pyrite and chalcopyrite (SNB 07 – E13, SNB 07 – E02A02, SNB 07 – E01A02-2; Plates 6 and 7).

MINERAL GEOCHEMISTRY

METHODS

Mineral compositions were obtained from thin sections by electron microprobe using a WDS-CAMECA SX 50 instrument at the Serveis Cientificotècnics of the Universitat de Barcelona (Spain). Excitation voltage was 20 kV and beam current 15 nA, except for analyses of Cr-rich spinel for which a current of 20 nA was preferred. Most elements were measured with a counting time of 10 s, except for Ni, V and Zn (30 s).

CHLORITE

The chlorite is penninite (Mg-rich chlorite; Table 1), which is close to the Mg-rich composition of the listvenite's protolith, as shown in Figure 2. The high Mg content of the chlorites is more typical of chlorites that are associated with ore-bearing rocks. However, their Si content is relatively low and falls within the field for hydrothermally altered rocks. This could be due to the precipitation of pyrite and magnetite that consume the FeO present in the system and force chlorites to more Mg-rich compositions.

CHLORITE THERMOMETRY

It is generally accepted that the composition of chlorite is related to the physicochemical conditions of formation. In the range 50 to 400°C, both the structure and the chemistry of the chlorite group changes from swelling varieties of trioctahedral character (smectite to mixed layers types) at lower grades to true chlorites (*sensu stricto*) at higher grades. Cathilenau (1988) demonstrated that the $^{[IV]}$Al content of chlorites in hydrothermally altered andesite increases with the temperature and can be used as a geothermometer. This change is accompanied by an increase in $^{[VI]}$Fe and a decrease in the octahedral vacancy. In addition to the Al–Si substitution, Fe–Mg substitution in chlorites reflects changes in temperature (Kranidiotis and McLean, 1987) and the oxygen and/or sulphur fugacity of the contemporaneous fluids.

Table 1: Chlorite compositions of the samples collected in this study

Sample	SiO_2	TiO_2	Al_2O_3	Cr_2O_3	FeO	MnO	MgO	CaO	Na_2O	K_2O	ZnO	NiO	$H_2O(c)$	Sum Ox%
A02-1-2	33.36	0	14.54	0.72	7.84	0	30.42	0	0.03	0	0.08	0.3	12.47	99.77
A02-1-3	33.14	0.03	14.06	0.53	9.12	0	30.22	0	0	0	0.07	0.22	12.4	99.78
A02-1-4	33.74	0	14.39	0.44	4.63	0.04	33.14	0	0	0	0	0.21	12.59	99.18
A02-1-5	32.63	0.01	14.79	0.37	7.17	0.02	31.35	0.01	0.02	0	0.05	0.28	12.41	99.12
A02-1-6	32.56	0.03	14.18	0.4	9.1	0	29.57	0	0.02	0	0.01	0.27	12.22	98.37
A02-1-7	38.46	0.02	12.63	0.26	6.94	0.03	31.3	0	0	0	0	0.21	13.04	102.91
A02-1-10	32.82	0.02	14.38	0.45	6.42	0	32.23	0	0.02	0	0.03	0.25	12.45	99.06
A02-1-11	32.93	0	14.33	0.52	6.53	0	31.93	0.01	0	0.01	0.01	0.31	12.43	99.02
A02-1-12	32.97	0.01	14.37	0.49	5.64	0.04	32.86	0.02	0	0.02	0.01	0.25	12.5	99.18
A02-1-13	32.96	0	14.81	0.51	5.7	0.02	32.35	0.01	0	0.01	0.04	0.26	12.51	99.19
A02-1-15	32.99	0.02	15.06	0.12	4.65	0.05	33.15	0.03	0	0.01	0	0.31	12.54	98.95
A01-1-21	30.79	0	15.81	1.41	7.69	0.01	29.19	0.04	0	0	0	0.67	12.14	97.77
A01-1-22	32.23	0.01	14.26	1.36	7.45	0.06	29.73	0.06	0	0.01	0.01	0.59	12.2	97.97

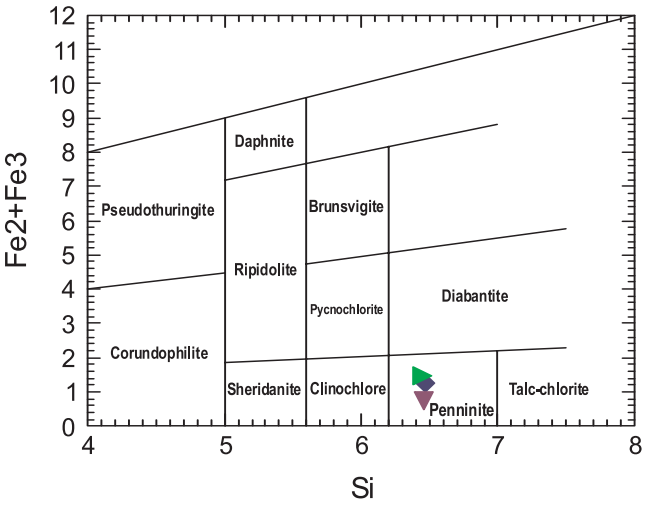

Figure 2. *Chlorite classification.*

The results from the application of various geothermometers to the chlorites analyzed are summarized in Table 2. It can be seen that the temperatures calculated using different calibrations differs by ~80°C in some samples. The Kranidiotis and MacLean (1987) geothermometer is better calibrated for highly magnesian chlorites such as those in this study (Table 2, column 4). Hence, the estimated temperature based on this thermometer is about 200°C. A critical assessment of the validity of the calculated temperatures may be achieved with the help of other independent methods, such as fluid-inclusion thermometry.

TALC

Talc is variably enriched in FeO (FeO>7.5 wt%). These compositions compare well with those of typical hydrothermal talc, which is often distinctly more iron rich than metamorphic talc and frequently shows distinct populations in a single site with either moderately or highly ferroan compositions (*e.g.*, Evans and Guggenheim, 1988; Shau and Peacor, 1992).

Table 2. Chlorite thermometry: 1) Cathelineau and Nieva (1985); 2) Cathelineau (1988); 3) Hiller and Velde (1991); 4) Kranidiotis and MacLean (1987); 5) Zang and Fyfe (1995)

Sample	1	1	2	3	4	5
A02-1-2	187	246	196	74	197	207
A02-1-3	188	263	196	74	198	206
A02-1-4	186	260	193	70	191	211
A02-1-5	199	271	214	102	208	221
A02-1-6	190	260	200	81	201	208
A02-1-7	118	170	90		126	139
A02-1-8	156	232	148		165	176
A02-1-9	212	288	233	132	217	238
A02-1-10	197	277	210	97	205	219
A02-1-11	195	271	207	91	203	217
A02-1-12	197	278	210	97	204	221
A02-1-13	197	268	211	98	204	221
A02-1-14	220	313	244	150	224	245
A02-1-15	199	271	214	102	205	224
A01-1-21	226	261	254	165	236	246
A01-1-22	199	247	213	101	208	219

CARBONATES

The carbonate minerals are dolomite, ankerite and magnesite (Table 3). Dolomite is generally associated with talc minerals and magnesite is associated with ankerite.

SULPHIDES

The major sulphide phase present in the studied sam-

Table 3. Carbonate compositions of the samples collected for this study

Carbonate Label	$FeCO_3$	$MnCO_3$	$MgCO_3$	$CaCO_3$	$SrCO_3$	Stonianite	Rhodochrosite	Magnesite	Siderite	Calcite	
E01-P3-15	14.68	0.18	82.41	0.22	0.02	0.011	0.143	88.211	11.432	0.196	MAGNESITE
E01-P3-16	10.12	0.08	90.05	0.08	0	0.002	0.059	92.318	7.55	0.072	MAGNESITE
E01-P3-19	1.95	1.47	41.81	51.51	0.25	0.165	1.228	47.594	1.612	49.4	DOLOMITE
E01-P3-20	18.26	0.12	87.74	0.17	0.01	0.006	0.089	86.645	13.119	0.14	MAGNESITE
E01-P3-21	2.66	0.06	42.95	51.82	0.17	0.111	0.05	48.411	2.181	49.211	DOLOMITE
E01-P3-22	14.36	0.46	81.26	1.06	0.01	0.007	0.36	87.428	11.244	0.962	MAGNESITE
B01-26	9.11	0.07	90.5	0.31	0.02	0.012	0.056	92.852	6.804	0.27	MAGNESITE
E13-28	31.93	0.59	67.6	0.25	0.04	0.024	0.473	73.872	25.39	0.235	MAGNESITE
E13-29	10.96	0.27	83.05	0.27	0.01	0.007	0.218	90.791	8.718	0.248	MAGNESITE

Plate 8. *Pyrite crystals.*

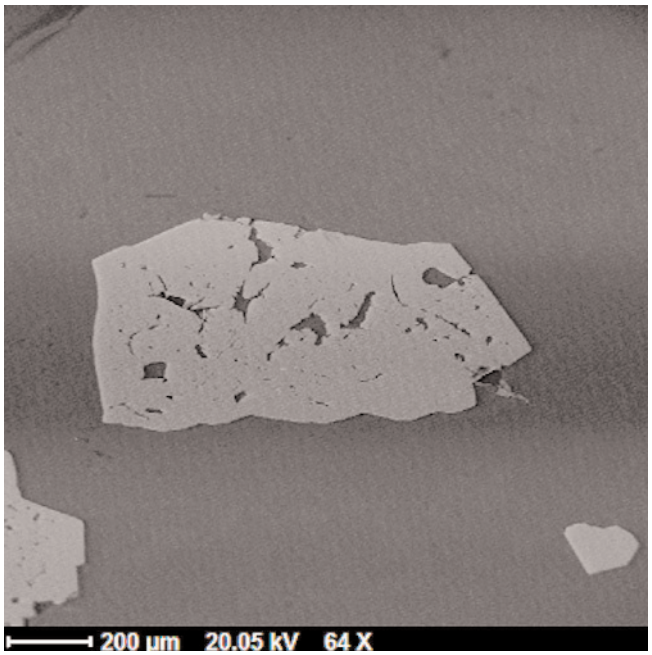

Plate 9. *Pyrite crystals in the listvenite.*

ples is pyrite (Plates 8 and 9) with inclusions of chalcopyrite and a third mineral rich in Au and Hg (Table 4) that is presently unidentified (Plate 10). The presence of a Hg–Au phase in pyrite suggests that epithermal mercury-precious-metal deposits may form an analogue for metasomatism and mineralization in the Point Rousse listvenites. Thompson and Thompson (1996) defined the silica–carbonate alteration, which is common in mercury and precious-metal deposits of epithermal type, as a low-temperature event formed by CO_2-rich springs in a wide stability field ranging between 17 and 200°C. Craig (1973) proposed temperatures below 200°C for the presence of pyrite and millerite in listvenites and related rocks (Auclair *et al.*, 1993). These data are consistent with the preliminary inferences from chlorite geothermometry.

SPINEL

Spinel is the only magmatic phase that is preserved in listvenites and has been shown to be a sensitive petrogenetic indicator in ultramafic rocks. Despite the generally high degree of alteration, spinel has retained relict cores. Relict cores show an intermediate composition with Cr# 0.60 (Plates 11 and 12). The borders are altered to ferrichromite and are enriched in Zn, in the samples where chromite is in contact with carbonate minerals such as magnesite and ankerite. In one sample (E01-P3-14; Table 5), the spinel has a magnetite composition (Plate 13). The Mg# is variable between 37 and 75 and plot within the array of depleted Izu–Bonin–Marians (IBM) SSZ peridotites. The incompatible oxide TiO_2 is low, less than 0.05%. The SSZ peridotites are characterized by spinels that have much higher Cr# than abyssal peridotites, which indicates significantly higher degrees of partial melting in the SSZ peridotites compared to abyssal peridotites. Models of partial melting at anhydrous conditions of 'fertile MORB mantle' (FMM) have shown that spinels with Cr# 0.60 are the response to ~30%

Table 4. Sulphide compositions. Samples with totals below 61% are arsenopyrite with Au mineralization; studies are ongoing

Label	S W%	Fe W%	Cu W%	Ag W%	Sn W%	Au W%	Hg W%	Pb W%	Sum W%
A02-1-p1	53.24	46.39	0	0.04	0.05	0	0	0.21	99.93
A02-1-pS1	52.92	46.45	0	0.03	0.01	0.01	0.17	0.12	99.71
A02-1-pS2	52.46	45.9	0	0.03	0.03	0	0	0.19	98.61
A02-1-pS3	53.3	46.87	0.12	0.01	0.06	0.05	0.04	0.15	100.6
A02-1-pS4	25.94	13.02	61.12	0.12	0.03	0.05	0	0.06	100.34
A02-1-pS5	34.72	30.59	34.29	0.06	0.02	0.06	0	0.12	99.87
A02-1-pS6	53.15	45.81	0	0.05	0.1	0.08	0	0.12	99.31
A02-1-pS7	31.61	29.13	0	0.06	0.04	0.22	0.08	0.04	61.17
A02-2-pS8	53.38	46.61	0	0.02	0.06	0	0	0.14	100.21
A02-2-pS9	53.6	46.22	0.02	0.03	0.05	0	0	0.15	100.08
A02-2-pS10	53.53	46.58	0.03	0.02	0.03	0.04	0	0.22	100.45
A02-2-pS11	17.09	3.71	0.01	0	0.01	0	0	0.03	20.85
A02-2-pS12	31.49	28.96	0	0.03	0.02	0.15	0	0.14	60.78
A02-2-pS13	34.79	30.99	34.28	0	0.02	0	0	0	100.09
A02-2-pS14	34.66	30.47	34.06	0.01	0.05	0.02	0	0.07	99.35
A02-2-pS15	53.53	46.43	0	0.03	0.05	0.01	0	0.12	100.18
A02-2-pS16	31.35	25.09	0.03	0.03	0.05	0.17	0	0.05	56.78
A02-2-pS17	31.6	25.09	0.05	0	0.07	0.28	0	0.14	57.23
A02-2-pS18	32.82	21.67	0.06	0.03	0.05	0	0	0.12	54.75
A02-2-pS19	53.69	46.66	0.02	0.04	0.04	0	0	0.18	100.63
A02-2-pS20	0.2	53.33	0.08	0	0.05	0	0.03	0.02	53.71
A02-2-pS21	34.82	30.96	34.22	0.02	0.04	0	0.04	0	100.09
A02-2-pS22	34.73	30.56	34.49	0.01	0.02	0	0	0.08	99.89
A02-2-pS23	53.14	45.45	0	0.03	0.04	0.02	0	0.21	98.9
A03-2-pS23	53.55	46.38	0	0.04	0.05	0.01	0.02	0.16	100.21
A03-2-pS24	0	34.79	0.04	0.06	0.06	0	0	0.03	34.99
A03-2-pS25	53.67	46.25	0	0.04	0.06	0	0	0.07	100.08
A03-2-pS26	33.57	28.75	33.31	0.05	0.03	0.14	0.02	0.13	96

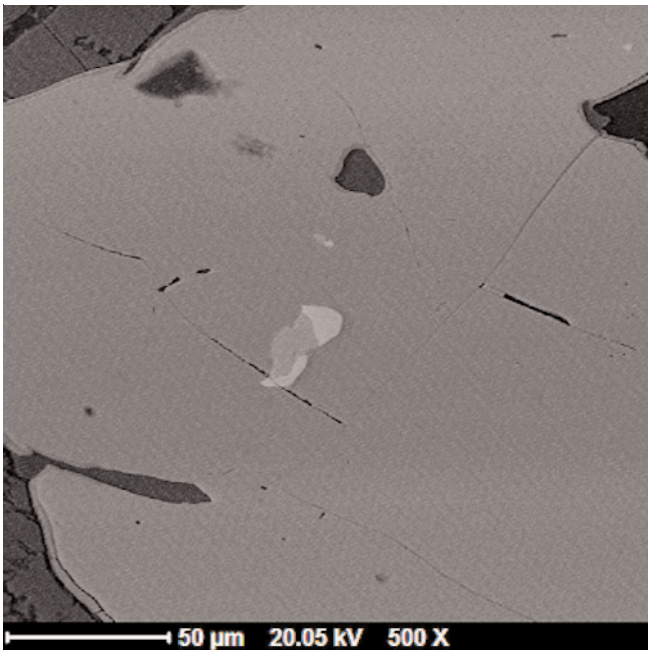

Plate 10. *Pyrite crystal with chalcopyrite and arsenopyrite inclusions.*

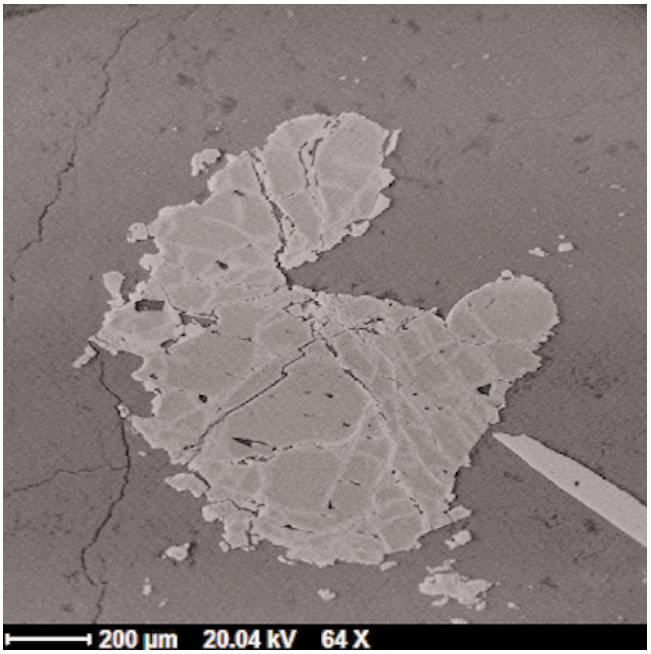

Plate 11. *Chromite with primary cores and ferrichromite rims.*

Table 5. Spinel compositions of the samples collected for this study

Label	MgO	Al_2O_3	SiO_2	TiO_2	VO_2	Cr_2O_3	MnO	FeO(t)	NiO	ZnO	Sum O
E-01-p2-1	5.55	21.47	0.08	0.04	0.24	45.04	0.15	27.46	0.1	0.58	100.72
E-01-p2-2	2.93	21.2	0.04	0.05	0.23	44.15	0.14	30.19	0.17	1.4	100.5
EP1-P2-3	2.26	20.93	0.04	0.02	0.16	43.57	0.12	29.39	0.08	3.26	99.83
4	1.13	16.62	0.06	0.03	0.17	42.49	0.15	34.11	0.07	3.32	98.15
E01-P2-5	2.04	19.46	0.06	0.01	0.24	45.11	0.14	29.21	0.06	3.36	99.69
E01-P2-6	0.57	11.05	0.05	0.02	0.23	43.26	0.22	39.64	0.13	2.08	97.25
E01-P3-11	2.6	19.81	0.06	0.02	0.24	44.53	0.11	31.37	0.13	1.64	100.5
E01-P3-12	1.0	16.52	0.09	0.0	0.26	43.45	0.14	34.52	0.08	3.29	99.34
E01-P3-14	0.0	0.0	0.04	0.37	0.13	0.54	30.52	66.51	0.06	0.05	98.22

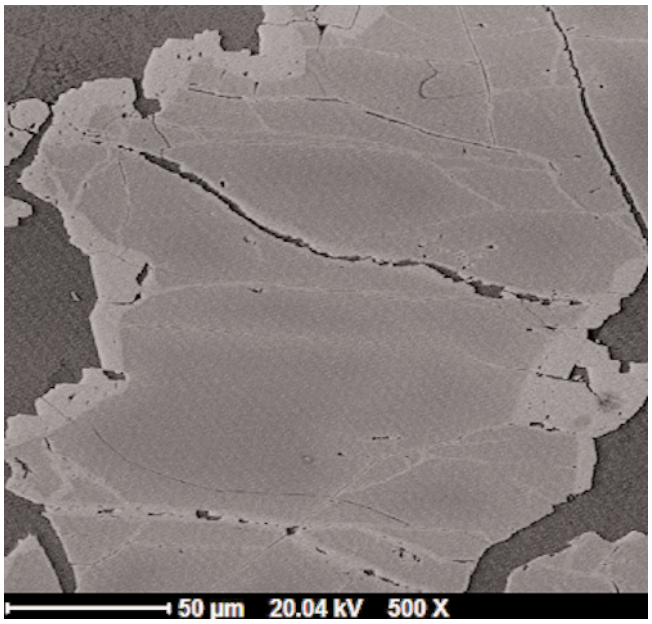

Plate 12. *Chromite with primary cores and ferrichromite rims.*

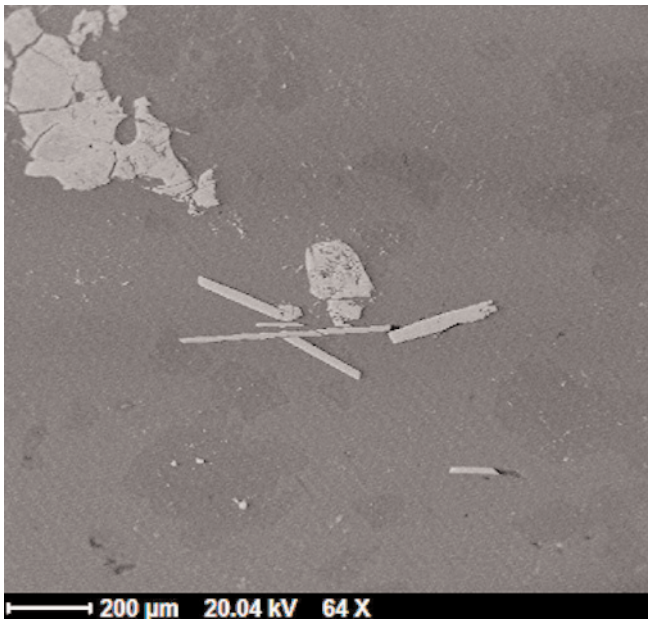

Plate 13. *Magnetite crystals.*

of batch melting. Thus, the chemical compositions of spinels in the Point Rousse listvenites are consistent with the formation of their ultramafic precursors in a SSZ forearc setting (Figures 3 to 6).

GENESIS OF ALTERATION

Several genetic models have been proposed to explain the formation of silica–carbonate alteration assemblages. These models require the presence of structural features such as thrusts, faults or a micro-fractured and porous host-rock, to provide conduits for the hydrothermal fluid input. These models also require specific physicochemical characteristics for the fluids. For example, the Eastern Metals Ni–Cu–Zn deposit in the Québec Appalachians required introduction of Ca, CO_2, S and As-rich solutions with low fO_2 and fS_2 and high temperatures (>350°C) to account for carbonatization, and high fO_2 and fS_2, combined with moderate to low temperatures to account for silicification (Auclair *et al.*, 1993).

The oxygen and sulphur fugacity (fO_2 and fS_2) are considered to be critical factors in the formation of sulphide phases during serpentinization following metasomatism. Frost (1985) proposed that CO_2-rich fluid infiltration into a primary peridotite at temperatures below 400°C can produce a significant amount of carbonate with a narrow margin of quartz and magnesite at the rims of the peridotite. He also noted that the oxygen fugacity will show a sharp rise in the carbonatized zone according to the extremely low-fO_2 conditions present at the serpentinization front. For a constant sulphur value in the rock, the fugacity of sulphur would vary sympathetically with that of oxygen. These arguments indicate that precipitation of sulphide species during the alteration requires high fO_2 as well as fS_2.

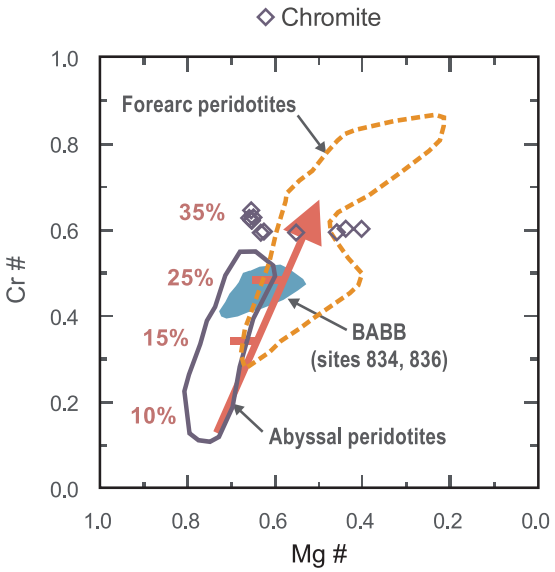

Figure 3. *Fields of different peridotite types are from compilation of Dupis* et al. *(2005). The arrow represents the percentage of melting of the host peridotite (Hirose and Kawamoto, 1995).*

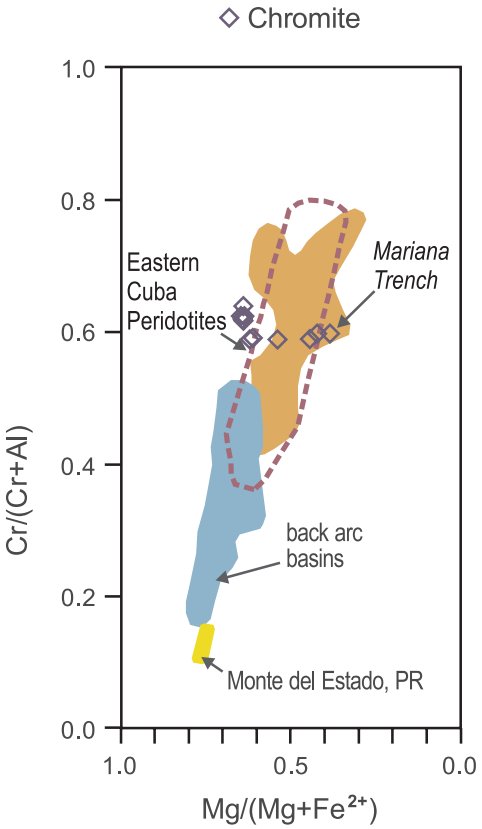

Figure 4. *Field for eastern Cuba peridotites (hazburgite and dunite) is from Proenza* et al. *(1999a, b) and Marchesi* et al. *(2006).*

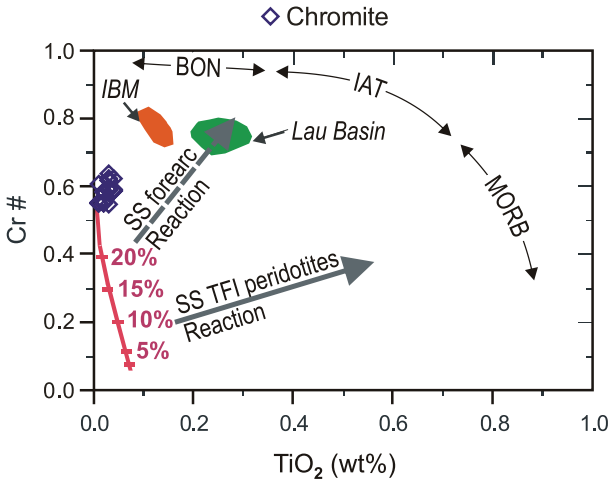

Figure 5. *Modified from Pearce* et al. *(2000). FMM – fertile MORB mantle; SS – South Sandwich; IBM – Izu–Bonin–Mariana; BON – Boninites; IAT – Island-arc tholeiites; SS TFI – South Sandwich Trench Fracture Zone intersection.*

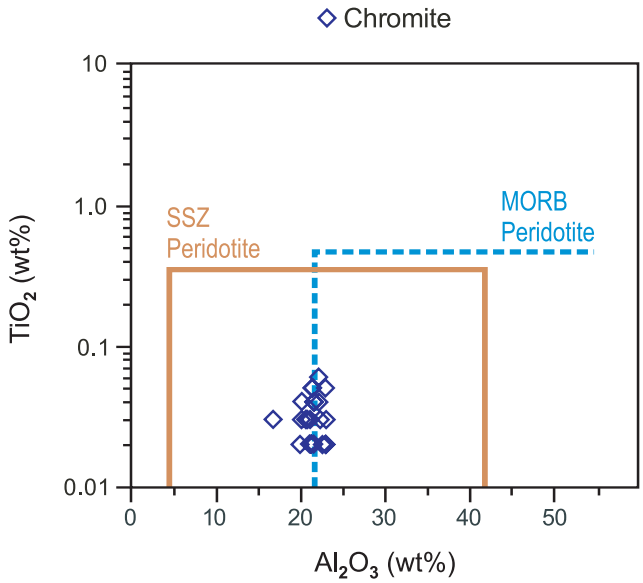

Figure 6. *Al_2O_3 values <20 wt% imply high degrees of mantle melting and are typical of spinels from SSZ mantle peridotites and island arc (Kamenetsky* et al., *2001).*

The pH and temperature of the fluid are also important factors that control the nature and crystallization of the alteration assemblages. Changes in these conditions create temporal and/or spatial phase differentiation. Silicon solubility increases in high-pH and high-temperature environments, so the silicification is achieved by a fluid with a lower pH and temperature during interaction with the wall rock. In contrast, the absence of silica indicates a higher pH and moderate to high-temperature fluid, which holds the silica in solution and facilitates carbonate precipitation.

There are various studies on the formation and temperature of the silica–carbonate assemblages. A maximum temperature range between 350 and 400°C is suggested for a stable quartz–dolomite assemblage at X_{CO2} varying between 0.1 and 0.5 at 1 kBar. Spiridonov (1991) determined a formation temperature ranging between 280 and 340°C in CO_2-rich fluid inclusions in larger quartz grains of listvenite-like metasomatic rocks associated with gold deposits of Armenia. Hansen *et al.* (2004) suggested that some listvenites can form directly from unserpentinized ultramafic rocks. In this model, assemblages of uncarbonatized antigorite + relict olivine, brucite and orthopyroxene are transformed to assemblages containing antigorite + magnesite + talc + quartz. However, the reaction sequence described in most studies of listvenites starts with serpentinization reactions that consume olivine + orthopyroxene to form serpentine + magnetite.

In the Point Rousse ophiolite, evidence for these reactions has not been observed in the studied samples. This could be explained by a major carbonatization front formed by a fluid with high temperature and pH that produces the complete destruction of antigorite and reacts to formation of a dolomite + talc + chlorite assemblage, or the carbonatization of an unserpentinized protolith in the manner suggested by Hansen *et al.* (2004). At lower temperatures, increase of fO2 and fS_2, and lower pH, leads to a new assemblage of quartz + magnesite + ankerite that overgrows the original alteration assemblage, whereas a further decrease in temperature leads to the precipitation of pyrite and other sulphides at about 200°C, as suggested by chlorite thermometry data.

MODEL OF OCCURRENCE

Deformation associated with obduction creates fractures that become pathways for externally derived hydrothermal fluids. High-temperature (>350 to 400°C), high-pH fluids rich in SiO_2, Ca and CO_2 flush through the faults and are forced upward through the fractures. Such process is typical of active hydrothermal fields in near-rift, off-axis settings and sediment-covered spreading centres.

Carbonatization of the rock takes place due to water-rock interaction, where Ca and CO_2-rich fluid reacts with Mg-rich host rocks. These reactions result in the formation of widespread dolomite. Frost (1985) indicates that high fO_2 conditions in a H_2S-rich fluid should decrease the solubility of sulphides and result in the precipitation of these phases. As sulphide-bearing assemblages are present in the carbonate-rich rocks in the study area, a fluid characterized by high fO_2 and H_2S-rich fluid at every stage of alteration is required, especially in the final silica-rich, low-temperature stages. The high fO_2 and fS_2 at decreasing temperatures (–250°C) promotes precipitation of magnetite and pyrite. The silica and pyrite–magnetite-rich metasomatic rocks are observed together in the field where they are associated with structures such as breccias and mylonites (Plate 14). Hence, we infer that deformation must be an important factor in focusing fluid flow during the last stage of alteration.

Plate 14. *Different stages of fluid intrusion. Note change of foliation and pyrite mineralization.*

CONCLUSIONS

Listvenites and related metasomatic rocks are the products of a hydrothermal system reacting with ultramafic rocks. They are important first-order exploration guides. Late-stage geological structures that could facilitate the remobilization of metals within the listvenites are important secondary controls. The metal content of the deposits in listvenites is dictated not only by the initial composition of the ultramafic rocks, but also by the surrounding rock units. Precipitation of the observed metallic mineral assemblages is mainly controlled by oxygen and sulphur fugacity variations under moderate to low temperatures. Gold present in trace amounts in ultramafic–mafic rocks is mobilized and deposited during hydrothermal alteration in sulphides and arsenides, and then re-precipitated in late-stage structures.

The Point Rousse listvenites were formed by the hydrothermal alteration and tectonic deformation of obducted ultramafic rocks and have much in common with listvenites described elsewhere. They should thus be considered a potential target for Cu–Au mineralization, and perhaps also for Zn and Ni, based on analogues in Québec. Despite widely varying morphologies, host rocks, and metallic mineral assemblages in this deposit class, all examples are intimately related to fault zones that bound slices and blocks of carbonatized ophiolitic ultramafic rocks.

The hydrothermal mineral assemblages in the Point Rousse listvenites are controlled largely by temperature,

X_{CO2}, and oxygen and sulphur fugacities. The transformation of the rocks to talc–carbonate schist (listvenite) by Ca-CO_2-S and As-rich solutions liberated important quantities of silica that were subsequently mobilized and re-deposited to form quartz-rich rocks and quartz vein networks. Similar silica–carbonate alteration in epithermal mercury and precious-metal deposits originates as a low-temperature event formed by CO_2-rich springs in a wide stability field ranging between 17 and 200°C. These data are consistent with the presented mineral associations and chlorite geothermometry and suggest that more studies must be developed in aim to discover Au mineralization associated to the Point Rousse listvenites origin.

ACKNOWLEDGMENTS

This work was supported by the Geological Survey of Canada Targeted Geoscience Initiative Program 3. This manuscript was improved by the review of Dr. Alex Zagorevski. We are grateful to Dr. Andy Kerr from the Newfoundland and Labrador Geological Survey whose suggestions improved this manuscript.

REFERENCES

Auclair, M., Gauthier, M., Trottier, J., Jebrak, M.and Chartrand, F.
1993: Mineralogy, geochemistry and paragenesis of the Eastern Metals serpentinite-associated Ni-Cu-Zn deposits, Quebec Appalachians. Economic Geology, Volume 88, pages 123-138.

Cathilenau, M.
1988: Cation site occupancy in chlorites and illites as a function of temperature. Clay Minerals, Volume 23, pages 271-346.

Craig, J.R.
1973: Pyrite-pentlandite assemblages and other low temperature relations in the Fe-Ni-S system. American Journal of Science, Volume 273-A, pages 496-510.

Dupuis, C., Hébert, R., Dubois-Côté, V., Guilmette, C., Wang, C.S., Li, Y.L. and Li, Z.J.
2005: The Yarlung Zangbo suture zone ophiolitic mélange (southern Tibet): new insights from geochemistry of ultramafic rocks. Journal of Asian Earth Sciences, Volume 25, pages 937-960.

Evans, B.W. and Guggenheim, S.
1988: Talc, pyrophyllite and related minerals. *In* Hydrous Phyllosilicates (Exclusive of Micas). *Edited by* S.W. Bailey. Reviews in Mineralogy, Mineralogical Society of America, Washington, DC, pages 225-294.

Frost, B.R.
1985: On the stability of sulfides, oxides, and native metals in serpentinite. Journal of Petrology, Volume 26, pages 31-63.

Guhtrie, G.D., Carey, J.W., Bergfeld, D., Byer, D., Chipera, S., Ziock, H. and Lackner, K.S.
2001: Geochemical aspects of the carbonation of magnesium silicates in an aqueous medium. Procedures of the First National Conference on Carbon Sequestration (Washington), Session 6C, 14 pages.

Halls, C., Zhao, R., Shine, C., Cooper, C. and Harrington, K.
1991: Listvenites and related rocks associated with gold mineralization in Co. Mayo, Ireland. Mineralogical Society of Great Britain and Ireland, Winter Conference, Cardiff, December 16-18, 1991, Industrial and Environmental Mineralogy, Programme and Abstracts, 25p.

Halls, C. and Zhao, R.
1995: Listvenite and related rocks: perspectives on terminology and mineralogy with reference to an occurrence at Cragganbaun, Co. Mayo, Republic of Ireland. Mineralium Deposita, Volume 30, pages 303-313.

Hansen, L.D., Dipple, G.M., Anderson, R.G. and Nakano, K.F.
2004: Geologic setting of carbonate metasomatised serpentinite (listvenite) at Atlin, British Columbia: implications for CO_2 sequestration and lode-gold mineralization. *In* Currrent Research. Geological Survey of Canada, 2004-A5, 12 pages.

Hansen, L.D., Dipple, G.M., Gordon, T.M. and Kellet, D.A.
2005: Carbonate serpentinite (listvenite) at Atlin, British Columbia: a geological analogue to carbon dioxide sequestration. Canadian Mineralogist, Volume 43, pages 225-239.

Hirose, K. and Kawamoto, T.
1995: Hydrous partial melting of lherzolite at 1 GPa: the effect of H_2O on the genesis of basaltic magma. Earth Planetary Science Letters, Volume 133, pages 463-473.

Kamenetsky, V.S., Crawford, A.J. and Meffre, S.
2001: Factors controlling chemistry of magmatic spinel: an empirical study of associated olivine, Cr-spinel and melt inclusions from primitive rocks. Journal of Petrology, Volume 42, pages 655-671.

Kranidioits, P. and McLean, W.H.
1987: Systematics of chlorite alteration at the Phelps

Dodge massive sulphide deposit, Matagami, Quebec. Economic Geology, Volume 82, pages 1898-1911.

Marchesi, C., Garrido, C.J., Godard, M., Proenza, J.A., Gervilla, F. and Blanco-Moreno
2006: Petrogenesis of highly depleted peridotites and gabbroic rocks from the Mayarí-Baracoa Ophiolitic Belt. Contributions to Mineralogy and Petrology, Volume 151, pages 717-736.

Pearce, J.A., Barker, P.F., Edwards, S.J., Parkinson, I.J. and Leat, P.T.
2000: Geochemistry and tectonic significance of peridotites from South Sandwich arc-basin system, south Atlantic. Contributions to Mineral Petrology, Volume 139, pages 36-53.

Proenza, J., Gervilla, F., Melgarejo, J.C. and Bodinier, J.L.
1999a: Al-rich and Cr-rich chromitites from the Mayarí-Baracoa ophiolitic belt (eastern Cuba): consequence of interaction between volatile-rich melts and peridotites in suprasubduction mantle. Economic Geology, Volume 94, pages 547-566.

Proenza, J., Gervilla, F., Melgarejo, J.C.
1999b: La /moho transition zone/ en el macizo ofiolitico Moa-Baracoa (Cuba): un ejemplo de interaccion magma/peridotita. /Revista de la Sociedad Geologica de Espana/, 12 (3-4), 309-327.

Rose, G.
1837: Mineralogisch-geognostiche Reise nach dem Ural, dem Altai and dem Kaspischen Meere. Volume 1: Reise nach dem sudlichen Ural und dem Altai. C.W. Eichhoff (Verlag der Sanderschen Buchhandlung). Berlin.

1842: Mineralogisch-geognostiche Reise nach dem Ural, dem Altai and dem Kaspischen Meere, Uebersicht der Mineralien und Gebirgsarten des Ural. Volume 2: Reise nach dem sudlichen Ural und dem Altai. C.W. Eichhoff (Verlag der Sanderschen Buchhandlung). Berlin.

Seifritz, W.
1990: CO_2 disposal by means of silicates. Nature, Volume 345, page 486.

Shau, Y.H. and Peacor, D.R.
1992: Phyllosilicates in hydrothermally altered basalts from DSDP Hole 504B, Leg 83 - a TEM and AEM study. Contributions to Mineral Petrology, Volume 112, pages 119-133.

Spiridonov, E.M.
1991: Listvenites and zodites. International Geology Review, Volume 33, pages 397-407.

Thompson, A.J.B. and Thompson, J.F.H.
1996: Atlas of Alteration: A Field and Petrographic Guide to Hydrothermal Alteration Minerals. Geological Association of Canada, Mineral Deposits Division, 240 pages.

Williams, H., Colman-Sadd, S.P. and Swinden, H.S.
1988: Tectonic-stratigraphic subdivisions of central Newfoundland. Paper - Geological Survey of Canada, 88-1B, pages 91-98.